HYDROLOGICAL PROCESSES
Hydrol. Process. (2012)
Published online in Wiley Online Library
(wileyonlinelibrary.com) DOI: 10.1002/hyp.9495

Multifractal behaviour of long-term karstic discharge fluctuations

D. Labat,[1]* C. T. Hoang,[2] J. Masbou,[1] A. Mangin,[3] I. Tchiguirinskaia,[2] S. Lovejoy[4] and D. Schertzer[2]

[1] *Géosciences Environnement Toulouse, Université de Toulouse-CNRS-IRD-OMP, Toulouse, France*
[2] *Université Paris EstEcole des Ponts ParisTech, CEREVEMarne-la-ValléeFrance*
[3] *CNRS, Moulis 09200, France*
[4] *Physics Department, McGill University, Montréal H3A 2T8, QC, Canada*

Abstract:

Karstic watersheds are highly complex hydrogeological systems that are characterized by a multiscale behaviour corresponding to the different pathways of water in these systems. The main issue of karstic spring discharge fluctuations consists in the presence and the identification of characteristic time scales in the discharge time series.
To identify and characterize these dynamics, we acquired, for many years at the outlet of two karstic watersheds in South of France, discharge data at 3-mn, 30-mn and daily sampling rate. These hydrological records constitute to our knowledge the longest uninterrupted discharge time series available at these sampling rates. The analysis of the hydrological records at different levels of detail leads to a natural scale analysis of these time series in a multifractal framework.
From a universal class of multifractal models based on cascade multiplicative processes, the time series first highlights two cut-off scales around 1 and 16 h that correspond to distinct responses of the aquifer drainage system. Then we provide estimates of the multifractal parameters α and C_1 and the moment of divergence q_D corresponding to the behaviour of karstic systems. These results constitute the first estimates of the multifractal characteristics of karstic spingflows based on 10 years of high-resolution discharge time series and should lead to several improvements in rainfall-karstic springflow simulation models. Copyright © 2012 John Wiley & Sons, Ltd.

KEY WORDS karst hydrology; multifractal analysis; scale analysis; time-series analysis

Received 16 December 2011; Accepted 4 July 2012

INTRODUCTION

The complex behaviour of karstic systems is mostly related to the coexistence of several pathways in water movements in these aquifers. Considering homogeneous porous aquifers, water both flows and is stored in the pores or in the fissures. Because of the low fluid velocity that keeps the flow laminar, this globally follows the classical Darcy law. The carbonate dissolution in karstic aquifers structure leads to an original hydrogeological structure that makes the water flow into large drains that are connected to peripheral systems that constitute large water reserves and where flows become turbulent. The existence of both rapid infiltration via boreholes and infiltration via epikarstic soil combined with diphasic flow in the unsatured zone and complex hydraulic connections in the saturated zone leads to a nonlinear discharge responses to rainfall input.

Because karstic watersheds are physically characterized by a multiscale behaviour, we propose here to provide a multifractal approach based on a short 30-mn rainfall time series and long and uninterrupted discharge time series at 3 and 30 mn sampling rate from 1995 up to the present period. This constitutes to our knowledge the longest uninterrupted discharge time series available at this fine sampling rate.

This contribution is organized as follows. First, we present a brief overview of the basics of spectral and multifractal analyses insisting on the incertitude of the parameter estimates. Then we present the results of the spectral and multifractal analyses first on daily data (but without illustrations because it mainly confirms previous results) and then on 30 and 3 mn sampling rate discharge time series measured at the outlet of the two watersheds.

Spectral and Multifractal analyses

In this part, we provide a brief overview of spectral and multifractal methods insisting on their applications in hydrology and also their scientific potential.

Classical spectral analysis consists in the interpretation of the variance density distribution (spectrum $S(\omega)$) across the scales (frequencies f or angular frequency ω). It essentially consists in the determination of frequency intervals on which the spectrum follows a power-law behaviour:

$$S(\omega) = \omega^{-\beta} \text{ for } \omega \in [\omega_1, \omega_2] \quad (1)$$

Equation (1) states that for any scaling field, there exists a log–log linear relation between frequency and power spectrum over a given range of frequencies

*Correspondence to: D. Labat, Géosciences Environnement Toulouse, 14 Avenue Edouard Belin, 31400 Toulouse, France.
E-mail: labat@get.obs-mip.fr

$[\omega_1,\omega_2]$. We here choose to implement multifractal analysis to make a more insightful analysis than the analysis presented in Labat *et al.* (2002). Multifractal analysis is an investigation method of the signal's scale-invariance properties first applied in hydrology to generate precipitation fields (Schertzer and Lovejoy, 1987; Lovejoy *et al.*, 1987; Hubert and Carbonnel, 1989; Lovejoy and Schertzer, 1990; Lavallée, 1991; Hubert *et al.*, 1993; Ladoy *et al.*, 1993; Olsson and Niemczynowicz, 1996; Svenson *et al.*, 1996; de Lima and Grasman, 1999; Biaou, 2004; Maramathas and Boudouvis, 2006; Royer *et al.*, 2008; de Lima and de Lima, 2009). These statistical techniques applied to rainfall and runoffs measured at the outlet of several watersheds already display characteristic time scales in their behaviour (Tessier *et al.*, 1996; Hubert, 1999; Pandey *et al.*, 1998; Zhou *et al.*, 2006). However, only a very limited number of hydrological investigations have focused on or considered karstic watersheds (Labat *et al.*, 2002; Majone *et al.*, 2004; Sauquet *et al.*, 2008), and for example, Majone *et al.* (2004) constitutes the only reference that already deals with this issue but really more restricted intervals corresponding to around 5000 successive hourly discharges.

Multifractal analysis consists in a more systematic investigation of the empirical moments of the signal as a function of the resolution. The observation of the behaviour of the empirical q-moments $M(\lambda, q) = \langle(\varepsilon_\lambda)^q\rangle$ function of the resolution $\lambda = L/l$ (where L is the total length of the signal and l is the length of the subinterval) and of the moment order q. Following Davis *et al.* (1994), the discrete dyadic process (rainfall or runoffs, here) noted here $\varphi(i)$ (with $i = 1,\ldots,2^N$) is first-order differentiated and then mean normalized to obtain new signals noted $\varepsilon_1(i)$. This signal is then aggregated on increasing size intervals of length $l = 2^m$ with $m = 1,\ldots,N$ with $L = 2^N$. At this time, we have at our disposal N discrete signals noted ε_λ, each one corresponding to a given resolution λ. Log–log representations of $M(\lambda,q)$ may then highlight power-law behaviour:

$$M(\lambda, q) \propto (\lambda)^{K(q)} \tag{2}$$

The $K(q)$ function defined in Equation (2) is typical of the multifractal analysis, and this method is called the Trace Moment method (Schertzer and Lovejoy, 1987). A theoretical model is required to correctly describe the $K(q)$ function, and the natural candidate is the "universal class of multifractals" for conservative processes based on Lévy stochastic variables. This model is the direct result of a multiplicative cascade structure (Schertzer and Lovejoy, 1987; Lovejoy and Schertzer, 1990) and is completely determined by two parameters α and C_1:

$$\begin{aligned} K(q) &= C_1 \frac{q^\alpha - q}{\alpha - 1}, \quad \text{for} \quad \alpha \neq 1 \\ K(q) &= C_1 q \log(q), \quad \text{for} \quad \alpha = 1 \end{aligned} \tag{3}$$

The parameter α is the Lévy index (also called the degree of multifractality) and lies in the interval [0,2]. It quantifies the distance of the process from monofractality: $\alpha = 0$ corresponds to a monofractal process, whereas $\alpha = 2$ corresponds to a lognormal multifractal process. The parameter C_1 characterizes the sparseness or inhomogeneity of the mean of the process. For example, concerning rainfall analysis, $K(q)$ 0 if the rainfall spatial distribution is homogeneous null or quasi-Gaussian

Another method of determining α and C_1 consists is the Double Trace Moment analysis developed by Lavallée (1991) and applied for example by Tessier *et al.* (1993). The Double Trace Moment analysis constitutes a generalization of the Trace Moment method developed. First, the discrete signals that can be noted as ε_1 corresponding to the highest resolution are elevated at a given η power ($\varepsilon_1{}^\eta$). Then the Double Trace Moment analysis is similar to the Trace Moment analysis but applied to the $\varepsilon_1{}^\eta$ discrete signals. The Double Trace Moment aims to exploit scale invariance of the q statistical moments of $\varepsilon_\lambda{}^{(\eta)}$ signals (obtained by aggregation of the $\varepsilon_1{}^\eta$ discrete signals) at lower and lower resolutions. The exponent of the power-law behaviour of the statistical moments satisfies

$$K(q, \eta) = \eta^\alpha K(q) \tag{4}$$

A log–log representation of $K(q,\eta)$ function of η allows the determination of the α multifractal parameter that corresponds to the linear part of the curve. The C_1 parameter can then be deduced from Equations (3) and (4) with $\eta = 1$. The determination of the multifractal α parameter is based on the inflection point method. The inflection point of the $K(q,\eta)$ function corresponds to the η value where the second derivative is equal to zero. That corresponds to the particular shape of the $K(q,\eta)$ mainly composed of two quasihorizontal parts corresponding to the lowest and highest η values. The parameter α corresponds to the first-order derivative at the inflection point. The Double Trace Moment analysis thus allows direct determination of the multifractal parameters α and C_1. The Trace Moment analysis then allows us to identify the multifractal behaviour of the moments and to determine the moment of divergence q_D.

In the universal multifractal concept (Schertzer and Lovejoy, 1987), the $K(q)$ function is a convex function, and the theoretical and empirical $K(q)$ functions are similar up to a given moment noted q_{crit} that constitutes the critical order of multifractal phase transitions. Then the empirical $K(q)$ function becomes linear for $q > q_{crit}$. Discontinuities in the first or second derivative of the $K(q)$ function corresponds to first-order or second-order multifractal phase transition (Schertzer and Lovejoy, 1992; Schertzer *et al.*, 1993). The order of the phase transition depends on the length of the signals. The first-order multifractal phase transition can only be observed if the length and number of series are sufficiently large and if $D + D_s > c(\gamma)$ where $c(\gamma)$ is the codimension. In this case, the critical moment q_{crit} correspond to the moment of divergence q_D. However,

DOI: 10.1002/hyp

when the length and number of signals is finite, but too small to obtain a first-order phase transition, the multifractal phase transition is of second order. Then the critical moment q_{crit} corresponds to the critical order q_S. In our case, the critical moment q_{crit} will be considered arbitrarily as equal to q_D (see Schmitt *et al.* (1994) for a discussion).

At this point, one can note that the determination of q_D is often based on the hyperbolic tail behaviour of the empirical probability distribution function of the series. However, this estimate leads to severe uncertainties relating to the interval of the variable on which the exponent is determined. This can lead for example to q_D larger than 20, which is not physically reasonable (Pandey *et al.*, 1998). Here, the moment of divergence q_D corresponds to the divergence between the experimental $K(q)$ function and the theoretical $K(q)$ function obtained by introducing the estimated multifractal parameters α and C_1 in Equation (3).

Results of the spectral and multifractal analyses

A high-resolution discharge measurement has been implemented on two karstic watersheds located in the French Pyrénées Mountains (Ariège) with a mean annual precipitation rate around 1650 mm. Aliou and Baget watersheds are two small basins with similar areas (around 13 km^2) and specific runoffs (36 l/s/km^2). Both watersheds can be considered as representative of high-developed to medium-developed karst systems over temperate climates (Figure 1) and already monitored but at daily sampling rate since 1968 (Labat *et al.*, 2000). Therefore, a preliminary investigation of daily discharge time series collected over more than 40 years (from 10/04/1969 up to 23/09/2011 for Aliou discharge time series and from 25/04/1968 up to 23/09/2011 for Baget discharge time series) mainly confirms the results obtained by Labat *et al.* (2000, 2002) on a more restricted time interval. We focus our attention on the high-resolution time-series analyses.

Spectral and multifractal analyses of daily hydrological data

First, we recall that daily precipitation exhibits spectral power-law behaviour with a slope equal to 0.47 (Labat *et al.*, 2000). Then when the hydrological signal is not filtered at all by the system (i.e. when the hydrological signal is rainfall), the slope tend to zero suggesting an uncorrelated signal at this sampling. The spectral analysis of daily discharge time series leads to

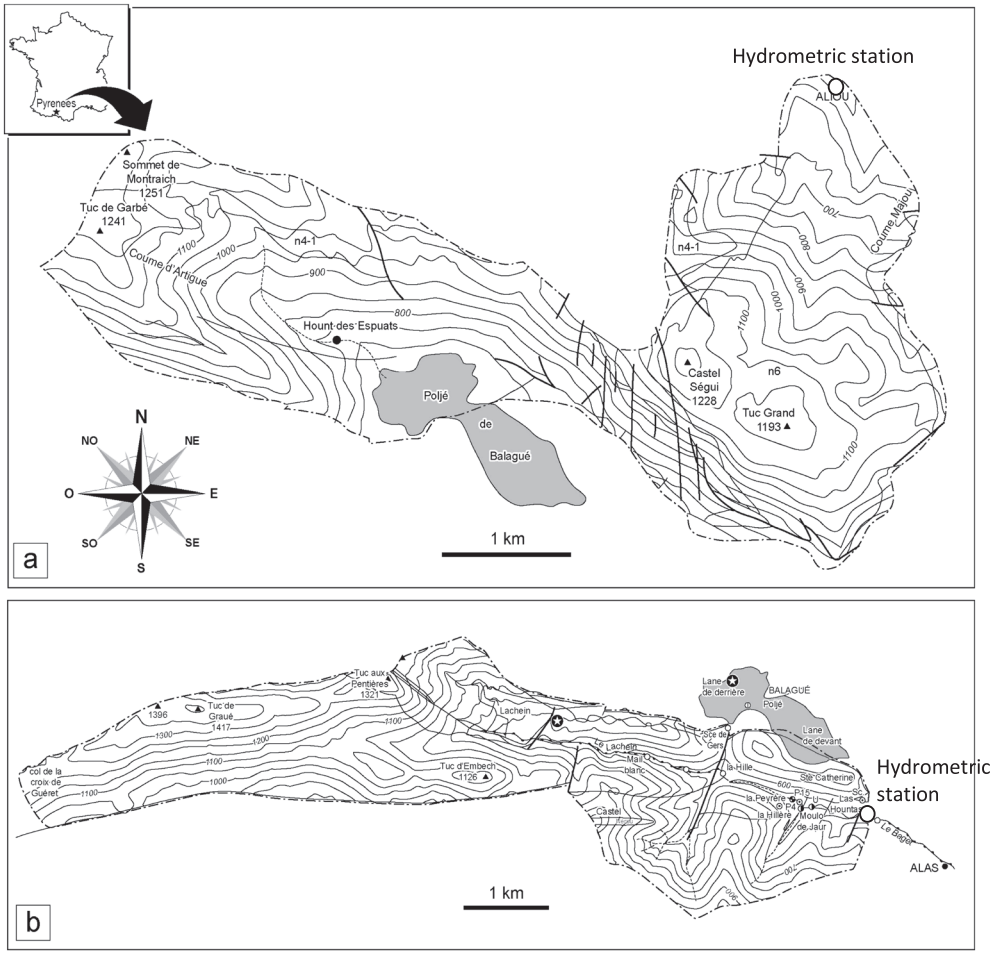

Figure 1. Localization of the Aliou and Baget karstic watersheds in the south of France with physiographic maps ((a) Aliou and (b) Baget). The circle indicates the position of the hydrometric station located at the outlet of the basin

DOI: 10.1002/hyp

the detection of a break in scale around 16 days for both watersheds with power-law behaviour for smaller scales than 16 days. This time scale is the transition between weather and low-frequency weather, and affects the precipitation statistics. The power-law behaviour on small scale processes is characterized by a slope $\beta = 1.25$ for Aliou discharge time series and $\beta = 1.89$ for Baget discharge time series. The increase of the slope of the spectral power-law behaviour is directly related to the decrease of the degree of karstification of the two aquifers. A less karstified aquifer leads to less abrupt floods and then leads to a more structured and autocorrelated temporal signal that corresponds to higher power-law slope. That increase of the power slope corresponds to a higher Hurst coefficient and then more fractional integration in the rainfall–discharge relationship based on Liouville integration point of view.

The Trace Moment analysis also leads to a break in scale around 16 days in accordance with the spectral analysis. With the Double Trace Moment method for high-frequency processes, the Levy index estimates are $\alpha = 1.55$ for Aliou watershed and $\alpha = 1.56$ for Baget watershed, and the intermittency indices are $C_1 = 0.27$ for Aliou watershed and $C_1 = 0.24$ for Baget watershed. The moment of divergence estimation based on the comparison between the experimental and theoretical $K(q)$ functions lead to $q_D = 2.0$ for Aliou watershed and $q_D = 1.8$ for Baget watershed. Therefore, the multifractal parameters α, C_1 and q_D appear to be close for both watersheds but with slightly lower C_1 value for the Baget watershed that corresponds to a lower degree of karstification that leads to lower intermittency in the discharge fluctuations and lower extreme discharges. These multifractal parameters appear as in good agreement with previous multifractal analyses of daily discharge time series such as Tessier *et al.* (1996) ($\alpha = 1.45 \pm 0.25$ and $C_1 = 0.2 \pm 0.1$), Pandey *et al.* (1998) ($\alpha = 1.65 \pm 0.12$ and $C_1 = 0.13 \pm 0.05$) and Zhou *et al.* (2006) ($\alpha = 1.63 \pm 0.19$, $C_1 = 0.11 \pm 0.02$ and $q_D = 4.44 \pm 0.60$). Therefore, at daily sampling rate, the karstic nature of these watersheds does not exhibit any particularity. We will now explore the multifractal behaviour of the hydrological time series at finer sampling rate.

Spectral and multifractal analyses of high-resolution hydrological data

We only have at our disposal a 30-mn rainfall time series over the time interval from 10/07/1993 up to 30/04/1996. The spectral analyses of the 30-mn discharge time series lead to a power-law behaviour with a break scale around 1 day. The Trace Moment analysis allows detecting a 16 h break scale with the following estimates of the multifractal parameters: $\alpha = 1.18$, $C_1 = 0.22$ and $q_D = 1.7$ for small scales and $\alpha = 0.79$, $C_1 = 0.35$ and $q_D = 1.8$ for large scales.

However, the main originality of our contribution lies in the first estimate of the spectral and multifractal parameters on long-term 30- and 3-mn sampling rate karstic spring discharge time series (Figure 2 and Table I: bg1, bg2 discharge time series for Baget spring and al1, al2 and al3 discharge time series for Aliou spring). Therefore, the error estimate for Aliou spring discharge spectral and multifractal parameters is based on three values (because we choose to consider that cut-off scales are close enough to be comparable), whereas the error estimate for Baget spring discharge spectral and multifractal parameters is based on two values.

The spectral analysis of Aliou and Baget 30-mn discharge time series (Figure 3) lead to the detection of power-law behaviour on two ranges of scales: from 1 h up to 1 day and from 1 day up to 1 month. Because we only have at our disposal three uninterrupted time series for Aliou watershed and two uninterrupted time series

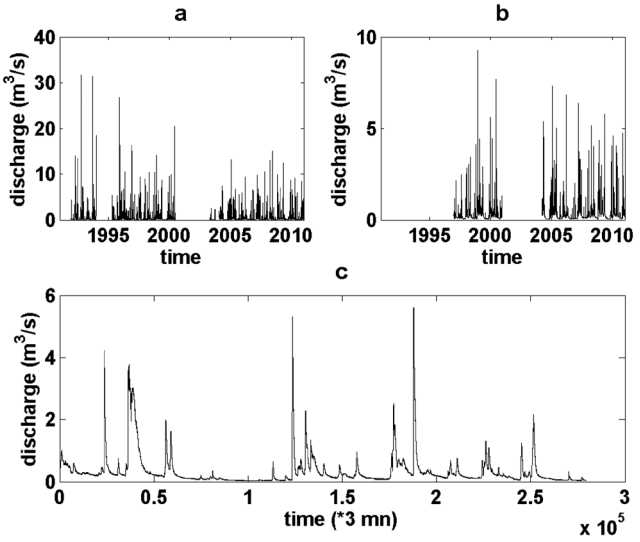

Figure 2. Visualization of the discharge time series: 30-mn sampling rate streamflow time series measured at the outlet of Aliou ((a) corresponding to the successive al1, al2 and al3 time series presented in Table I) and Baget ((b) corresponding to the bg1 and bg2 time series presented in Table I) and 3 mn high-resolution streamflow time series measured at the Baget station and corresponding to the bghres time series presented in Table I

DOI: 10.1002/hyp

Table I. Results of the multifractal analysis of the different 30 and 3 mn sampling rate discharge measured at the outlet of Baget and Aliou watersheds

Name	From	To	Number of data	α	C_1	q_D	α	C_1	q_D
30 mn Bagets spring discharge									
bg1	18/12/1996	09/12/2000	69 714	1,35	0,15	2,7	1,98	0,21	2,1
bg2	11/03/2004	23/09/2011	13 1979	1,49	0,19	2,1	1,25	0,30	2,5
30-mn Aliou spring discharge									
al1	29/11/1991	27/12/1993	36 341	1,06	0,12	1,9	1,41	0,42	2,1
al2	21/04/1995	27/06/2000	90 912	1,31	0,13	2,0	1,35	0,35	2,0
al3	27/01/2001	23/09/2011	134 125	1,48	0,11	2,7	1,17	0,33	2,0
3-mn Baget spring discharge									
bghres	17/02/2010	23/09/2011	279244	0,90	0,32	1,8	1,56	0,08	2,0

Concerning the 30 mn discharge time series, the first of multifractal parameters α, C_1 and q_D are estimated on the [30-mn;16-h] scale interval, whereas the second set of multifractal parameters are estimated on the [16-h;1-month] scale interval.
Concerning the 3 mn discharge time series, the first of multifractal parameters α, C_1 and q_D are estimated on the [3-mn;1-h] scale interval, whereas the second set of multifractal parameters are estimated on the [1-h;1 month] scale interval.

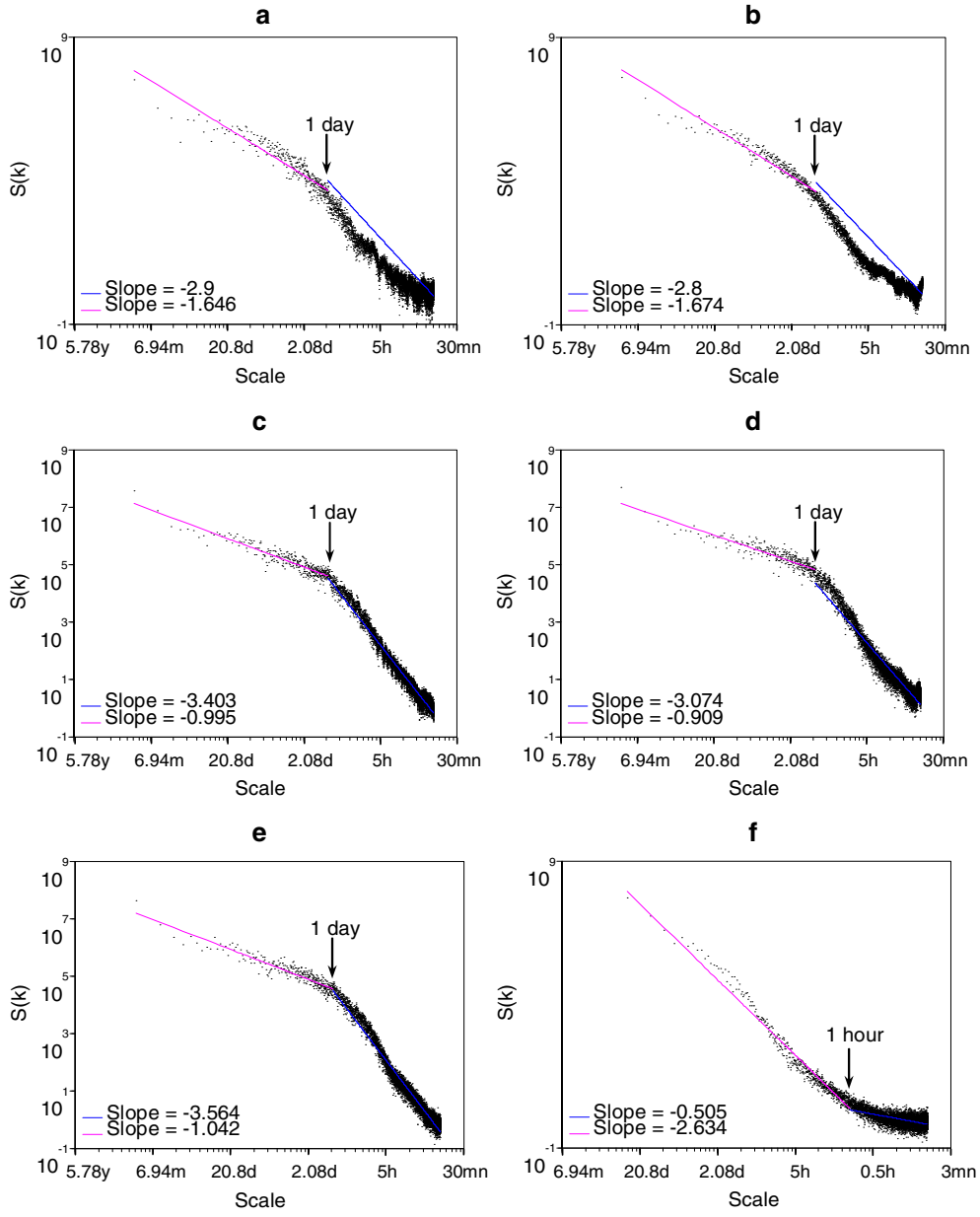

Figure 3. Log–log representation of the power spectra $S(k)$ of the discharge time-series function of the scale k. The straight lines have been fitted by regression and correspond to power-law behaviour in the spectra ((a) bg1 discharge series; (b) bg2 discharge series; (c) al1 discharge time series; (d) al2 discharge time series; (e) al3 discharge time series; and (f) bghres discharge time series)

DOI: 10.1002/hyp

for Baget watershed, we indicate the mean slope and the different slopes obtained for the different time series. The estimate of the slope of the power-law behaviour for the two scale ranges leads to the following estimates: for scales from 1 h to 1 day, $<\beta> = 3.35$ for Aliou watershed ($\beta = 3.40$ for al1, $\beta = 3.08$ for al2 and $\beta = 3.56$ for al3) and $<\beta> = 2.85$ for Baget watershed ($\beta = 2.90$ for bg1 and $\beta 2.80$ for bg2); for larger scales than 1 day, $<\beta> = 0.98$ for Aliou watershed ($\beta = 0.99$ for al1, $\beta = 0.90$ for al2 and $\beta = 1.04$ for al3) for Aliou watershed and $<\beta> = 1.66$ for Baget watershed ($\beta = 1.65$ for bg1 and $\beta = 1.67$ for bg2).

Therefore, the spectral analysis of the 30-mn discharge time series does not display significant differences for a given watershed considering nonoverlapping time intervals. The slight differences are not sufficiently high to be related to either nonstationarities in the hydrological response or climate change influence from our point of view.

The multifractal analyses of the discharge time series will now be displayed more precisely. The Figure 4a for example shows $M(\lambda, q) = \langle(\varepsilon_\lambda)^q\rangle$ function of the resolution λ (lambda) for the bg1 time series for values of q between 0.25 and 3.0. The curves exhibit a straight-line behaviour over two ranges of scales: from 30 min to 32 h and from 32 h to 21 days that correspond to the highest scale considered in the Trace Moment analysis. In the curves, on each interval, the straight lines have been fitted by regression. From the slopes of the lines in Figure 4a, one can estimate the empirical and discrete $K(q)$ function displayed in Figures 6a and 7a for values of q between 0.25 and 3.0. As previously mentioned, to

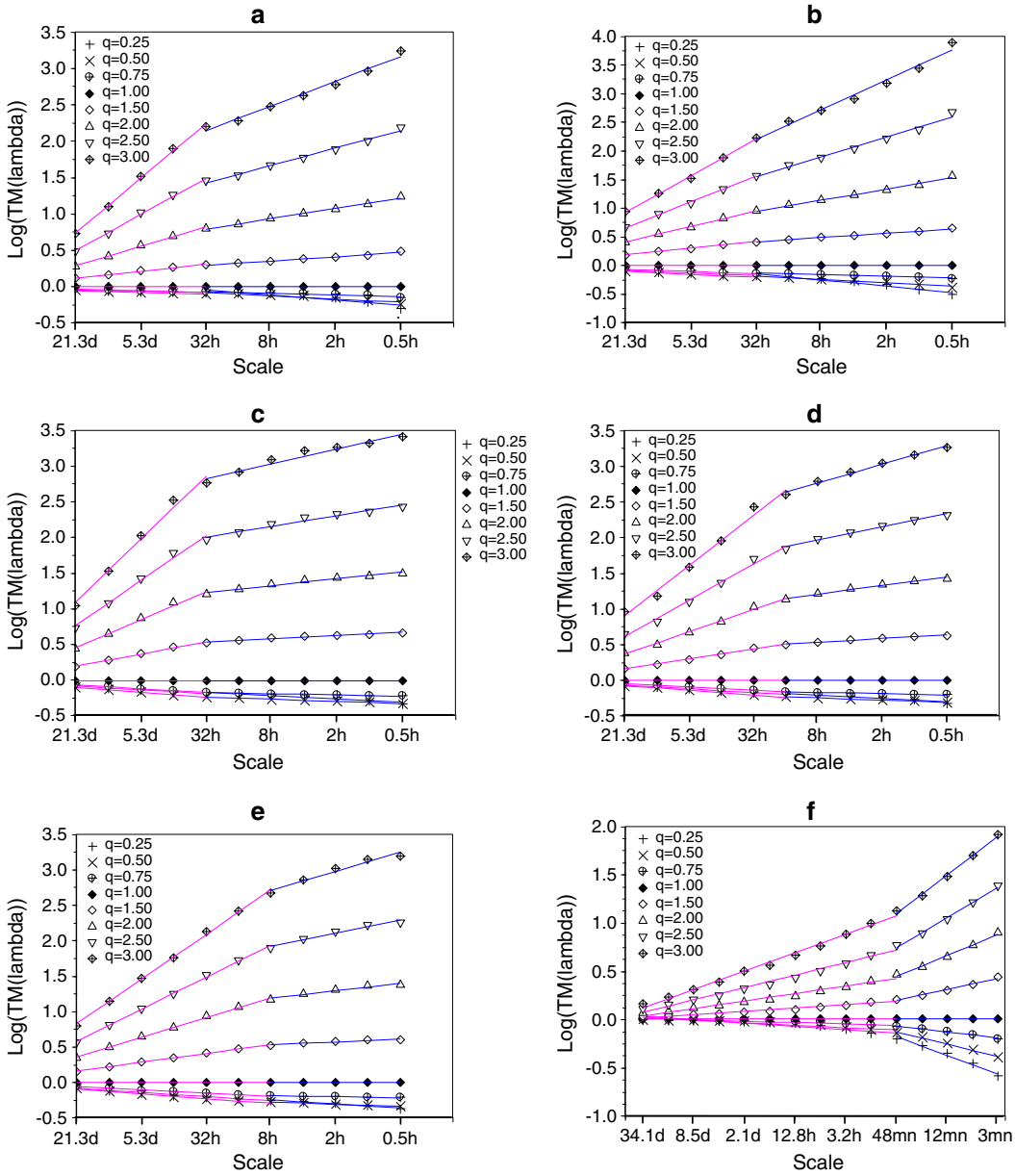

Figure 4. Average moment $M(\lambda, q) = \langle(\varepsilon_\lambda)^q\rangle$ function of the resolution λ (lambda) for values of q between 0.25 and 3.0. The straight lines have been fitted by regression. ((a)–(f): see Figure 3)

DOI: 10.1002/hyp

estimate the multifractal parameters α and C_1, the Double Trace Moment analysis is employed. The Figure 5a shows $K(q,\eta)$ for $q=1.5$, and the curve exhibits a straight-line behaviour for a given range of η and for both range of scales determined by the Trace Moment analysis. At both ends of the η intervals, the curve deviates from straight-lined behaviour, and the range of values of η over which the straight-line behaviour is observed is quite narrow.

The Trace Moment analysis allows determining several cut-off scales in the scale-invariance behaviour of the moment of the discharge time series. The 30-mn Baget spring discharge time series are characterized by two cut-off scales around 32 h and 21 days for the bg1 time series, whereas these cut-off scales are not as evident when analysing the bg2 time series. The 30-mn Aliou spring discharge time series are characterized by cut-off scale decreasing from 32 h for al1 to 16 h for al2 and finally 8 h for al3. We then consider a common break in scale for the 30-mn discharge different time series of 16 h to compare properly the multifractal estimates. At small scales, the multifractal parameter estimates are $\alpha=1.42\pm0.10$, $C_1=0.18\pm0.02$ and $q_D=2.40\pm0.07$ for Baget spring discharge time series and $\alpha=1.28\pm0.21$, $C_1=0.12\pm0.01$ and $q_D=2.20\pm0.44$ for Aliou spring discharge time series at small scales. For larger scales, the multifractal parameters estimates are $\alpha=1.62\pm0.52$, $C_1=0.26\pm0.06$ and $q_D=2.30\pm0.28$ for Baget spring discharge time series and $\alpha=1.31\pm0.13$, $C_1=0.37\pm0.05$ and $q_D=2.03\pm0.06$ for Aliou spring discharge time series.

Finally, the 3-mn discharge time series measured at the outlet of the Baget watershed over more than 1 year is analysed by spectral and multifractal analyses (Figures 3(f), 4(f), 5(f), 6(f) and 7(f)). The spectral

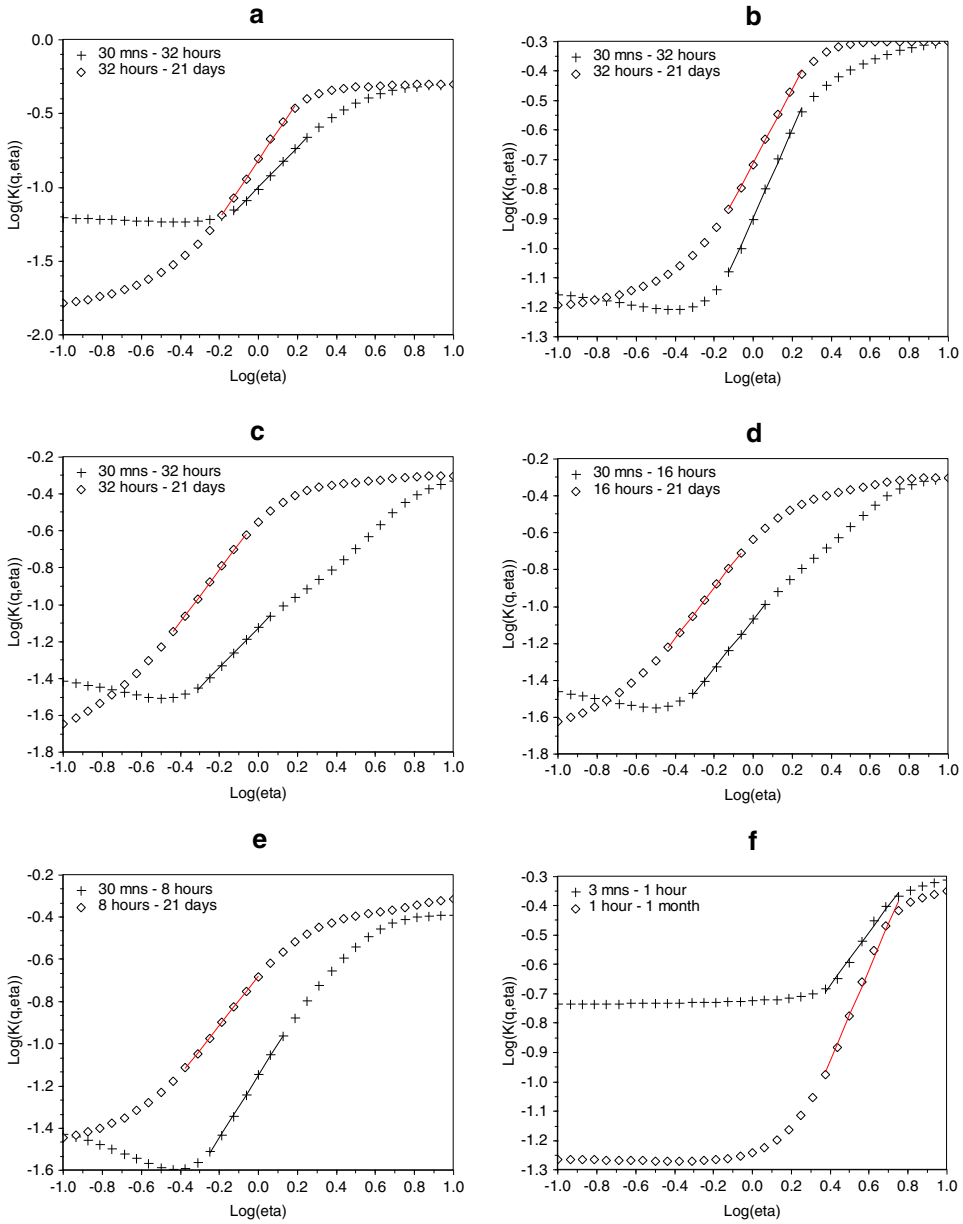

Figure 5. Double Trace Moment analysis: $K(q,\eta)$ as a function of η (eta) for $q=1.5$ for small and large scales. The straight lines, which have been fitted by regression, allow to determine the parameter α ((a)–(f): see Figure 3)

DOI: 10.1002/hyp

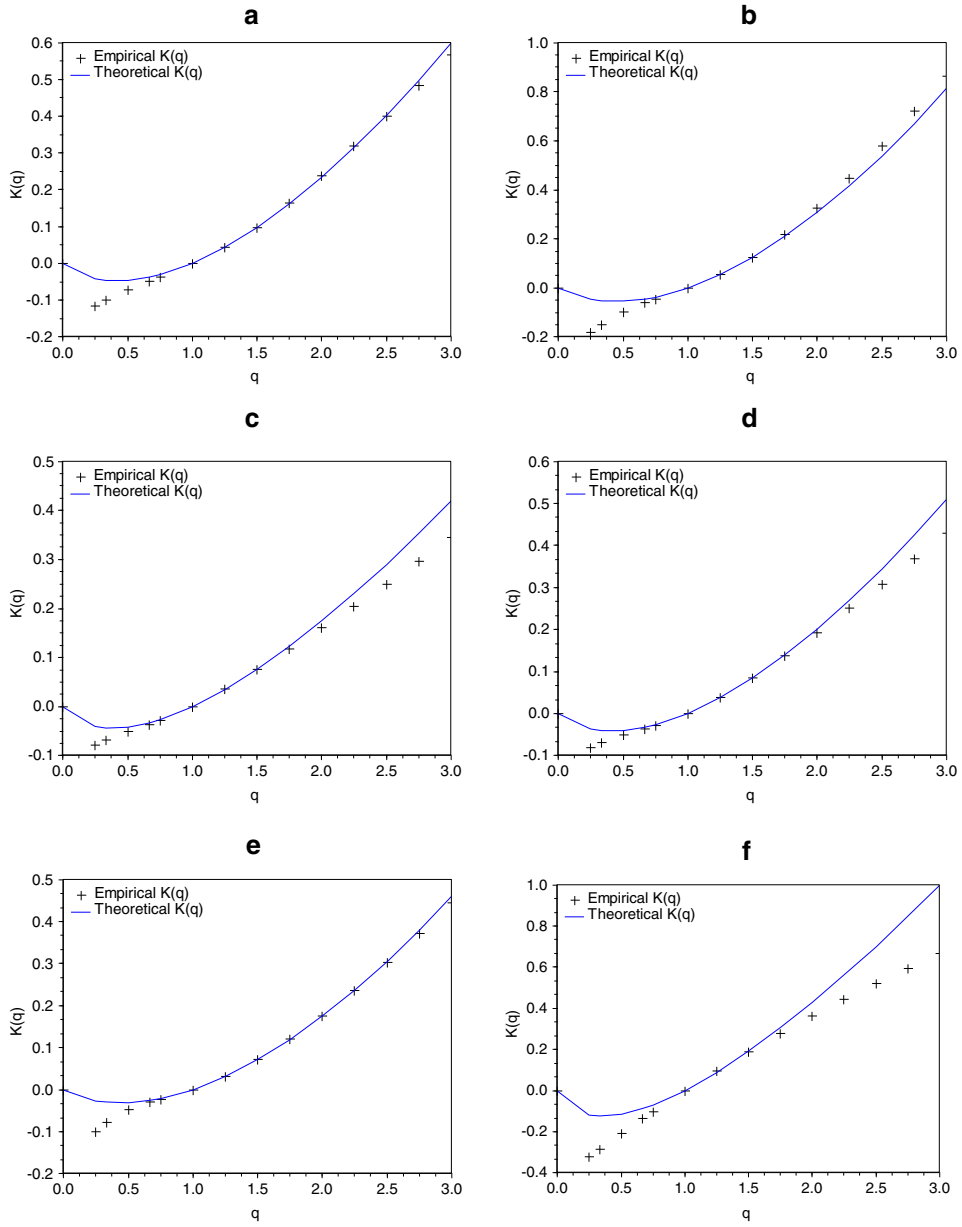

Figure 6. Moment scaling function $K(q)$ for the small scales obtained from the average moment analysis. The moment of divergence q_D corresponds to the q value where theoretical and empirical $K(q)$ functions exhibit significant differences ((a)–(f): see Figure 3)

analysis of Baget spring discharge 3 mn time series highlights slopes $\beta = 0.51$ for small scales (from 6mn to 1 h) and $\beta = 2.63$ for large scale (from 1 h to 1 month). That corresponds to a Hurst coefficient $H \approx 0$ at small scales and $H = 0.88$ at large scales. The Trace Moment analysis of high-resolution Baget spring discharge time series allows identifying a 1 h cut-off scale. With the Double Trace moment analysis, the 3-mn Baget spring discharge time series is characterized by the following multifractal parameters: $\alpha = 0.90$, $C_1 = 0.32$ and $q_D = 1.80$ for small scales (from 3 min to 1 h) and $\alpha = 1.56$, $C_1 = 0.08$ and $q_D = 2.0$ for larger scales (from 1 h to 1 month). The multifractal analysis of the 3-mn Baget discharge time series constitutes the first estimates of α, C_1 and q_D at this high-resolution sampling rate. We acknowledge that for the moment, the interpretation of α, C_1 and q_D still remain difficult, but we think that these results deserve to be compared with future analyses on comparable high-resolution discharge time series but on different hydrological watersheds.

CONCLUSION

This contribution allows the first determination of the multifractal parameters of 3- and 30-mn long-term karstic discharge and confirms the multifractal parameters estimation of karstic daily discharge fluctuation at the outlet of two karstic French systems.

The multifractal behaviour of karstic spring discharges is shown with a cut-off scale around 8 to 32 h. The multifractal parameters α, C_1 and q_D are quite

DOI: 10.1002/hyp

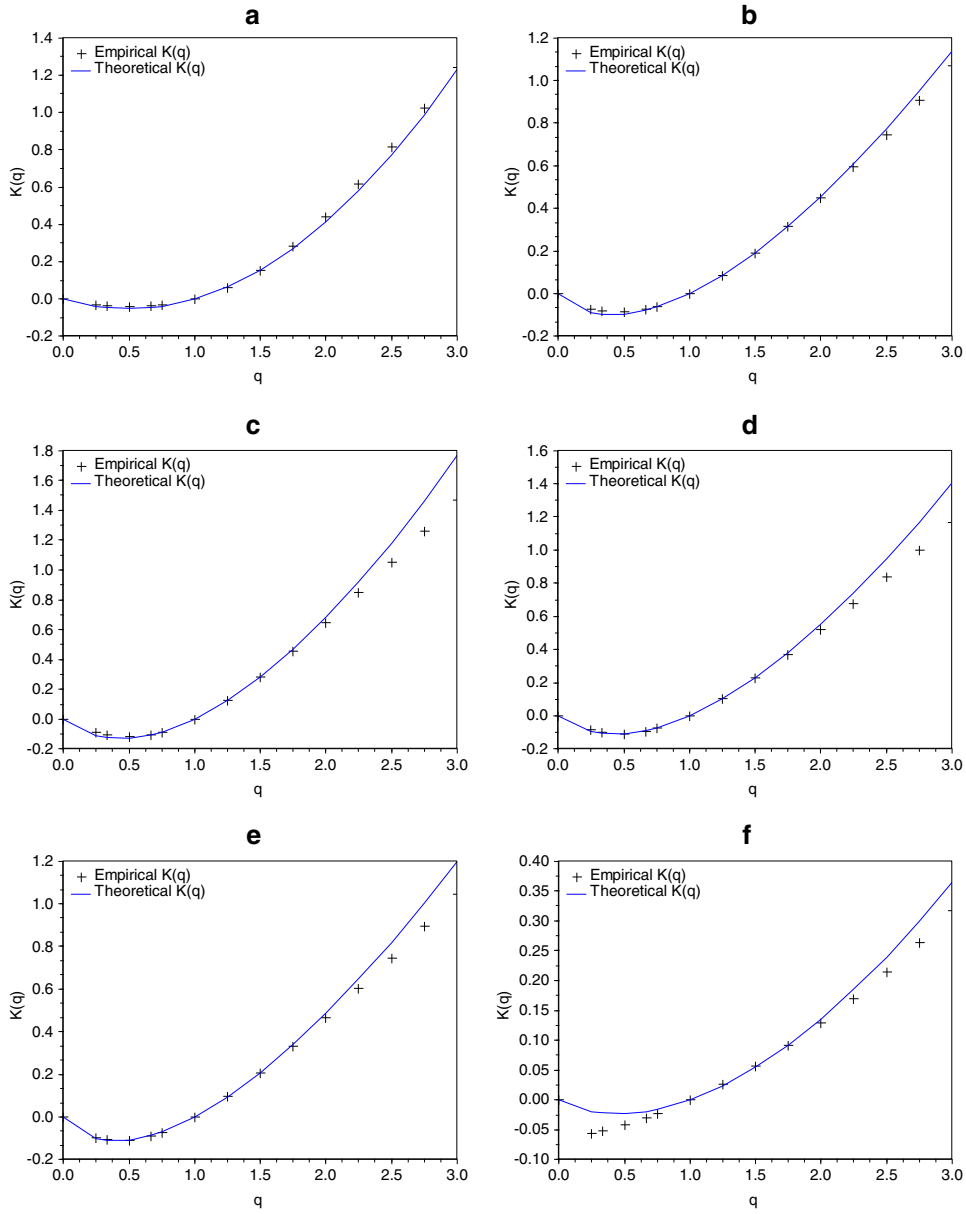

Figure 7. Moment scaling function $K(q)$ for the large scales obtained from the average moment analysis. The moment of divergence q_D corresponds to the q value where theoretical and empirical $K(q)$ functions exhibit significant differences ((a)–(f): see Figure 3)

different from Majone *et al.* (2004), but that may be related to both climate and the degree of karstification. Karstic systems must be considered as complex systems with a wide range of spatial and temporal scales in the runoff response. The multifractal framework constitutes in our point of view a unified concept that proposes a valuable alternative to the apparent complexity, exhibiting global invariant properties. This multifractal nature of the karst response is supposed to be linked to the fractal nature of the cave drainage network and karstogenesis models. Therefore, further karst watershed modelling must include this multifractal property well known in surface drainage network and also concepts such as multifractal instantaneous unit hydrograph (Gaudio *et al.*, 2004) or application of Liouville fractional integration (Tessier *et al.*, 1996) that deserved to be explored in karst hydrology.

REFERENCES

Biaou AC. 2004. De la méso-échelle à la micro-échelle: désagrégation spatio-temporelle multifractale des précipitations. PhD thesis, Ecole de Mine de Paris, Paris, 197 pp.

Davis A, Marshak A, Wiscombe W, Cahalan R. 1994. Multifractal characterizations of nonstationarity and intermittency in geophysical fields: observed, retrieved or simulated. *Journal of Geophysical Research* **99**(D4): 8055–8072.

Gaudio R, De Bartolo SG, Primavera L, Gabriele S, Veltri M. 2004. Lithologic control on the multifractal spectrum of river networks. *Journal of Hydrology* **327**(3–4): 365–375.

Hubert P. 1999. Des crues et des échelles. *La Houille Blanche* **8**(7): 83–87.

Hubert P, Carbonnel JP. 1989. Dimensions fractales de l'occurrence de pluie en climat soudano-sahélien. *Hydrologie Continentale* **4**(1): 3–10.

Hubert P, Tessier Y, Lovejoy S, Schertzer D, Schmitt F, Ladoy P, Carbonnel JP, Violette S, Desurosne I. 1993. Multifractals and extreme rainfall events. *Geophysical Research Letters* **20**(10): 931–934.

Labat D, Ababou R, Mangin A. 2000. Rainfall-runoff relations for karstic springs: continuous wavelet analysis and multiresolution analyses. *Journal of Hydrology* **238**: 149–178.

DOI: 10.1002/hyp

Labat D, Mangin A, Ababou R. 2002. Rainfall–runoff relations for Karstic springs: multifractal analyses. *Journal of Hydrology* **256**: 176–195.

Ladoy P, Schmitt F, Schertzer D, Lovejoy S. 1993. Variabilité temporelle multifractale des observations pluviométriques à Nîmes. *C. R. Acad. Sci. Paris, Ser* **317**: 775–782.

Lavallée D. 1991. Multifractal techniques: analysis and simulation of turbulent fields. PhD thesis, McGill University, Montreal, Canada.

de Lima MIP, de Lima JLMP. 2009. Investigating the multifractality of point precipitation in the Madeira archipelago. *Nonlinear Processes in Geophysics* **16**: 299–311.

de Lima MIP, Grasman J. 1999. Multifractal analysis of 15-min and daily rainfall from a semi-arid region in Portugal. *Journal of Hydrology* **220**: 1–11.

Lovejoy S, Schertzer D. 1990. Multifractals, universality classes and satellite and radar measurements of clouds and rain fields. *Journal of Geophysical Research* **95**: 2021–2034.

Lovejoy S, Schertzer D, Tsonis AA. 1987. Functional box-counting and multiple elliptical dimensions in rain. *Science* **235**(4792): 1036–1038.

Majone B, Bellin A, Borsato A. 2004. Runoff generation in karst catchments: multifractal analysis. *Journal of Hydrology* **294**(1–3): 176–195.

Maramathas AJ, Boudouvis A. 2006. Manifestation and measurement of the fractal characteristics of karst hydrogeological formations. *Advances in Water Resources* **29**: 112–116.

Olsson J, Niemczynowicz J. 1996. Multifractal analysis of daily spatial rainfall distributions. *Journal of Hydrology* **187**: 29–43.

Pandey G, Lovejoy S, Schertzer D. 1998. Multifractal analysis of daily river flows including extremes from basin of five to two million square modelling, one day to 75 years. *Journal of Hydrology* **208**: 62–81.

Royer JF, Biaou A, Chauvin F, Schertzer D, Lovejoy S. 2008. Multifractal analysis of the evolution of simulated precipitation over France in a climate scenario. *Comptes Rendus Geosciences* **340**(7): 431–440.

Sauquet E, Ramos M-H, Chapel L, Bernardara P. 2008. Streamflow scaling properties: investigating characteristic scales from different statistical approaches. *Hydrological Processes* **22**: 3462–3475.

Schertzer D, Lovejoy S. 1987. Physical modelling and analysis of rain and clouds by scaling multiplicative processes. *Journal of Geophysical Research* **92**(D8): 9693–9714.

Schertzer D, Lovejoy S. 1992. Hard and soft multifractal processes. *Physica A: Statistical Mechanics and its Applications* **185**(1–4): 187–194.

Schertzer D, Lovejoy S, Lavallée D. 1993. Generic multifractal phase transitions and self-organized criticality. *Cellular Automata: Prospects in Astrophysical Applications*, Perdang JM, Lejeune A (eds). Proceedings of Han-sur-Lesse Colloquium, Octobre 1992 (World Scientific, 1993), p. 268, World Scientific; 216–227.

Schmitt F, Schertzer D, Lovejoy S, Brunet Y. 1994. Empirical study of multifractal phase transitions in atmospheric turbulence. *Nonlinear Processes in Geophysics* **1**(2/3): 95–104.

Svenson C, Olsson J, Bernedtsson R. 1996. Multifractal properties of daily rainfall in two different climates. *Water Resources Research* **32**(8): 2463–2472.

Tessier Y, Lovejoy S, Schertzer D. 1993. Universal multifractal: theory and observations for rain and clouds. *Journal of Applied Meteorology* **32**(2): 223–250.

Tessier Y, Lovejoy S, Hubert P, Schertzer D, Pecknold S. 1996. Multifractal analysis and modelling of rainfall and river flows and scaling causal transfer functions. *Journal of Geophysical Research* **101** (D21): 26427–26440.

Zhou X, Persaud N, Wang H, Lin H. 2006. Multifractal scaling of daily runoff time series in agricultural watersheds. *Journal of the American Water Resources Association* **42**(6): 1659–1670.

DOI: 10.1002/hyp